HYBRID TESTING OF A PRESTRESSED GIRDER BRIDGE TO RESIST WAVE FORCES

Christopher Higgins[1], Jora Lehrman[2], Christopher Bradner[2],
Thomas Schumacher[2], and Daniel Cox[1]

Abstract

This paper describes hybrid tests to characterize the structural performance of connection details for prestressed girder bridges subjected to hurricane wave loading. Full-scale specimens were tested under dynamic cyclic forces using measured force time-histories from hydraulic tests of a 1/5 scale model of a highway bridge spanning a coastal embayment. The wave load effects included combined dynamically applied horizontal and vertical forces on the connections. Test results showed none of the connections considered would be capable of resisting newly specified vertical wave forces for large wave heights when significant air is entrapped under the bridge.

Introduction

The US has many bridges located in coastal regions that are susceptible to wave forces. Many of these bridges were not designed to resist the lateral and vertical forces from large wave loading. This has been demonstrated by recent strong hurricanes that have caused significant damage to the transportation infrastructure. Damage to bridges is of particular concern because these critical assets limit capacity of the transportation system and can delay rescue, recovery, and rebuilding efforts after an event.

Post disaster surveys by Douglass *et al*. (2006), Padgett *et al*. (2008), Robertson *et al*. (2007), and Chen *et al*. (2009) among others described the failure modes, costs, and the wave conditions surrounding the failed superstructures. Failures were attributed to storm surge allowing the surface waves to strike the superstructure and overcome the capacity of the anchorages. Subsequent waves pushed the superstructures off of the supporting substructure. Chen *et al*. (2009) and Douglass *et al*. (2006) both developed models to hind-cast the conditions along the Gulf Coast, determine the surge height, maximum significant wave height, wave period, and estimated the total forces acting on the bridge superstructures.

Previous experimental research regarding wave loads on structures (Denson.(1980), Bea *et al*. (2001), and Cuomo *et al*. (2007) has focused on off-shore drilling platforms which differ significantly from near-shore bridge superstructures. More recent experimental work was conducted by Marin and Sheppard (2009) utilizing a 1:8 scale model of the I-10 bridge over Escambia Bay, Florida. The study

---

[1]Professor and [2]Former Graduate Student, School of Civil and Construction Engineering, Oregon State University, Corvallis, OR 97330

experimentally determined inertia and drag coefficients for wave loads, and developed predictive equations for wave induced loading. These equations were the basis of the AASHTO *Guide Specification* (2008) for bridges vulnerable to coastal storms. While typical wave loading on bridges as well as the global failure modes have been investigated, the behavior of the individual structural connections between the superstructure and substructure has not been examined and realistic multi-axis force interactions have not been considered.

Research Significance

Presently, no data are available that characterize the structural performance of connections between the bridge superstructure and substructure under hurricane-induced wave loads. These are the connections that were reported to have failed in previous storms and thus may control survival of low-lying coastal bridges. The present research combines hydraulic tests of a 1:5 scale model of a real highway bridge located in Escambia Bay, Florida to measure the wave forces on the bridge. The research developed for the first time an innovative laboratory setup that allowed the test specimen to simulate the dynamic response of the superstructure. The measured wave force histories on the large-scale hydrodynamic model were converted into the vertical and horizontal force components at the connections. The force histories from the large-scale hydrodynamic model were increased to prototype scale and then applied dynamically to full-size connection elements to characterize the structural performance. This approach represents a new technique in hybid testing to investigate fluid-structure interactions and is applicable to tsunami research.

Hydrodynamic Model Test

The hydraulic experiments were conducted in the Large Wave Flume (LWF) at the O.H. Hinsdale Wave Research Laboratory at Oregon State University. The LWF is 104 m (342 ft) long, 3.66 m (12 ft) wide and 4.57 m (15 ft) deep. For these experiments, the bathymetry was comprised of an impermeable 1:12 slope, followed by a horizontal section approximately 30 m (98 ft) in length, and then another 1:12 slope to dissipate waves and minimize reflection off the beach. The specimen was located in the horizontal section, approximately 18 m (59 ft) landward of the offshore sloped bathymetry, and 46 m (151 ft) from the wavemaker as illustrated in Fig. 1.

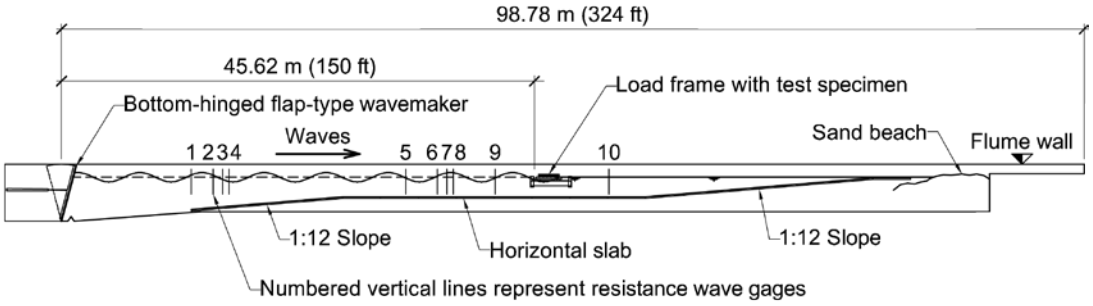

FIG. 1 – ELEVATION VIEW OF LARGE WAVE FLUME WITH SETUP.

The test specimen was based on prototype dimensions taken from Florida Department of Transportation drawings of the I-10 Bridge over Escambia Bay. Six scaled AASHTO Type III girders including the full complex cross-sectional geometry were constructed and connected with twin steel rods through four diaphragms spaced along the span. An analysis of the bridges damaged during Hurricane Katrina found that the individual spans failed independently, with little interaction between adjacent spans (NIST, 2006). This independent failure facilitated the testing of a single superstructure section. A geometric scale of 1:5 (undistorted) was chosen to allow the largest possible test specimen with a representative length to span the width of the wave flume. The total span length, S, of the model was 3.45 m (11.3 ft), the width, W, 1.94 m (6.36 ft), and the overall height, (h_d), 0.28 m (0.92 ft). Table 1 lists the model and prototype dimensions and weight. The deck was fastened to the girder and diaphragm sub-assemblage using 13 mm (0.5 in.) diameter threaded rods. Prior to installing the specimen in the wave flume, the gaps between the deck and supporting girders and diaphragms were sealed with caulking to replicate the air-tight integrity of the monolithically-cast prototype superstructures. Figure 2 shows the test specimen beams and diaphragms before attachment of the deck.

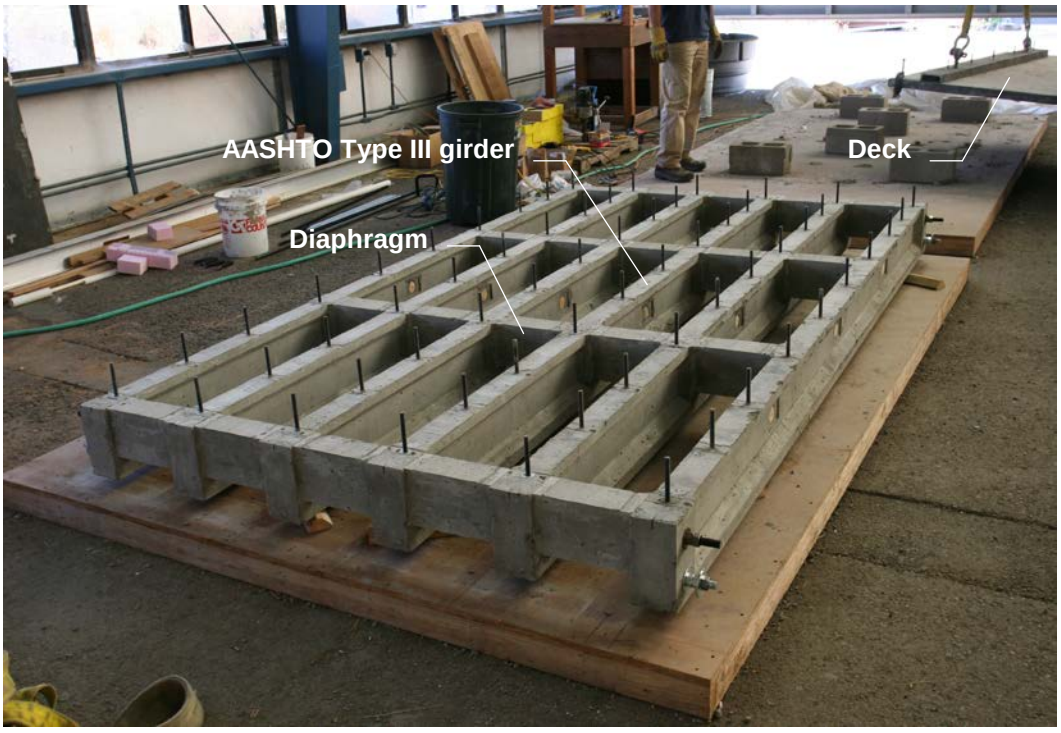

FIG. 2 – SPECIMEN ASSEMBLAGE OF GIRDERS AND DIAPHRAMS BEFORE PLACEMENT OF DECK.

Table 1. Properties of model test specimen (without guard rail) and corresponding prototype bridge.

Test parameter	Symb.	Model (1:5)	Prototype (1:1)
Water depth	H	1.60 - 2.17 m (5.25 – 7.12 ft)	8.0 – 10.9 m (26.2 – 35.6 ft)
Bottom girder clearance to SWL	d_c	± 0.279 m (± 0.92 ft)	±1.4 m (± 4.6 ft)
Wave height [1]	H	0.25 - 1.0 m (0.82 to 3.28 ft)	1.25 - 5.0 m (4.1 to 16.4 ft)
Significant wave height [2]	H_s	0.375 - 1.0 m (1.23 to 3.28 ft)	1.9 - 5.0 m (6.2 to 16.4 ft)
Wave period [1]	T	2.0 - 4.5 s	4.5 – 10.1 s
Peak wave period [2]	T_p	2.0 - 3.0 s	4.5 – 6.7 s

[1] For regular wave trials [2] For random wave trials

To simulate the dynamic response of the superstructure, a unique reaction frame was designed to permit the test specimen to move freely along the axis of wave propagation. The specimen was supported by two HSS7x5x1/2 steel members representing the bent caps. Each bent cap was then supported by two load cells mounted in line with the external offshore and onshore girders to measure vertical forces at these points. The four load cells were mounted on high-precision ball bearing rollers that allowed low friction motion of the load cells, bent caps and specimen along linear guide rails attached to the top flange of two W18x76 steel profiles (h = 0.50 m) bolted to each side of the flume wall. To measure horizontal forces, load cells were mounted between the offshore end of the bent caps and end anchorage blocks that were bolted to the flume wall. The specimen and reaction frame were mounted in the wave flume so that the bottom of the girders was located 1.89 m (6.2ft) above the horizontal bed to correspond with typical mudline-to-superstructure distances of the failed bridges. A drawing of the setup can be seen in Fig. 3

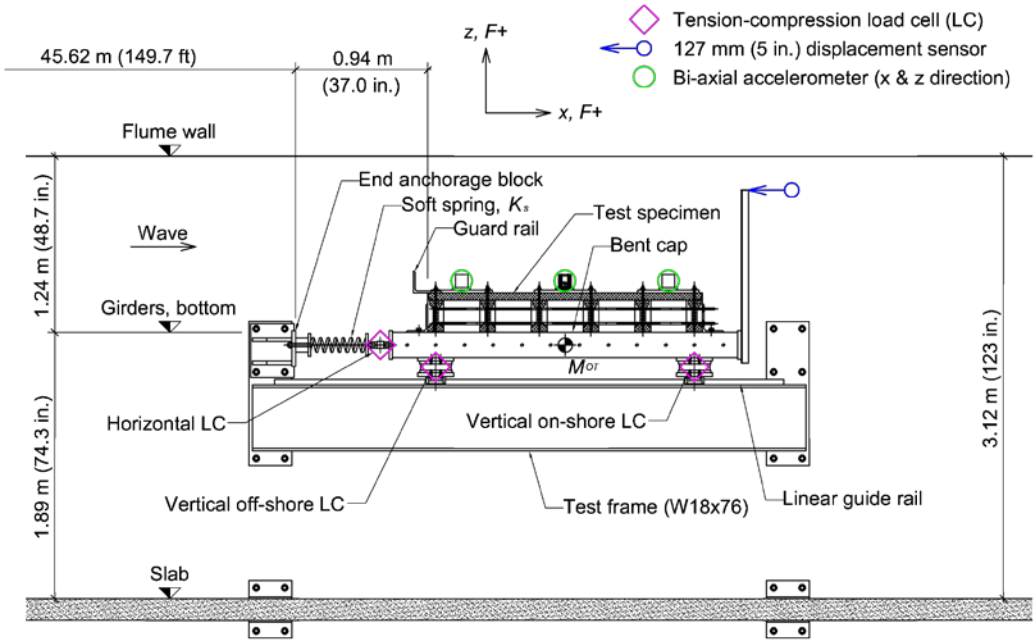

FIG. 3 - ELEVATION VIEW OF TEST SPECIMEN (FLEXIBLE SPRING SHOWN).

To investigate the influence of substructure flexibility on the wave loading response, an adjustable dynamic setup was developed and integrated into the reaction frame. The flexibility of the prototype substructure was modeled by a pair of elastic springs installed between the bent caps and the end anchorage blocks. To determine the required spring stiffness for the model, a finite element (FE) analysis was performed on a prototype-scale bridge similar in design to the test specimen. Two sets of springs were investigated. The first set was designed to be relatively soft in order to deliberately exaggerate displacements. The second, stiffer set of springs was chosen to realistically represent the bridge substructure. The two sets of springs selected for this project had spring constants of 107 kN/m (612 lb/in.) and 458 kN/m (2614 lb/in.) which produced fundamental periods of 0.95 s and 0.46 s, respectively.

The hydraulic experiments were divided in three phases. Phase 1 simulated a rigid structure. The test specimen was bolted to the bent caps and each bent cap was then connected to an end anchorage block via a load cell. Phase 2a and 2b simulated a flexible substructure using the previously described medium and soft springs, respectively. The springs were added to the bent cap-end anchorage block linkage described above, allowing the specimen and bent caps to vibrate along the rail guide (see Fig. 3). Phase 3 was designed to simulate the response of the bridge span upon failure of the bent cap connections. For this phase, the bent caps were rigidly connected to the end anchorages as in Phase 1, but the test specimen was disconnected from the bent caps with only the specimen self-weight and the resulting friction providing resistance.

Wave conditions and water levels were designed to simulate realistic conditions found at coastal bridges along the Gulf of Mexico during extreme events. Typically

these bridges are located in shallow water of 3-10 m (10-33 ft) and are somewhat protected by shoals and barrier islands. As a result, waves at these bridges are considerably smaller in height and length relative to ocean waves. Even during catastrophic events such as Hurricane Katrina, numerical modeling by Chen, et al. 2009) estimates a relatively small maximum significant wave height of 2.6 m (8.5 ft) and a peak period of 5.5 s at the U.S. 90 Bridge over Biloxi Bay. Similar conditions have been reported for Hurricane Ivan at the I-10 Bridge over Escambia Bay. Using the conditions hindcast by these models as a guide, a realistic range of water levels, wave heights, and wave periods was developed. To simulate storm surge, the water depth, h, at the specimen was adjusted from 1.61 m (5.3 ft) to 2.17 m (7.1 ft) in increments of 0.14 m (5.5 in.) which is equal to one-half the specimen height. The resulting SWL ranged between 0.28 m (11 in.), below the bottom of the girders to even with the top of the deck. A non-dimensional parameter, $d^* = (h-z_d)/h_d$, that represents the SWL elevation relative to the bottom of the girders, where z_d is the elevation of the bottom flange above the mudline and h_d is the height of the bridge deck. For these experiments, values of d^* ranged from -1.0 to +1.0 in increments of 0.5. For each of the five water depths, regular and random wave conditions were tested. For the regular wave trials, target wave height (H) and period (T) ranged from 0.25 to 1.0 m (0.8 to 3.3 ft) and 2.0 to 4.5 s respectively. Random wave trials consisted of a series of approximately 300 waves with a TMA spectrum (γ = 3.3). Target significant wave height (H_s) and peak period (T_p) ranged from 0.375 to 1.0 m (1.2 to 3.3 ft) and 2.0 to 3.0 s respectively. In all, 428 trials were conducted and the test variables are shown in Fig. 4.

The sensor suite was designed to measure wave conditions, forces and pressures acting on the specimen, and the response of the specimen as shown in Fig. 5. To measure water surface elevation, 10 surface piercing resistance wave gages (WG) were placed along the length of the flume (see Fig. 1). Gages 1-8 were arranged into two arrays of four and positioned offshore of the specimen to resolve incident and reflected waves at two locations. Gage 9 was placed approximately 4 m (13 ft) offshore of the specimen to measure water surface elevation in the vicinity of the specimen and Gage 10 was located 6 m (20 ft) onshore of the specimen. Six tension-compression load cells were deployed to measure overall forces on the model. Four ±89 kN (±20 kip) capacity load cells were mounted between the bent caps and rollers on the linear guide rail to measure vertical forces. The remaining two load cells were ±44 kN (±10 kip) capacity load cells that measured horizontal forces acting at mid-height of the bent caps. All six load cells were calibrated in the actual test configuration. To measure pressure distribution, 13 pressure transducers were installed in the specimen. Steel mounting plates were cast into the concrete so that the sensors could be securely flush-mounted to the surface of the specimen, minimizing the disruption of flow as well as the sensor response due to vibration. Pressure sensors were mounted in the offshore face of the deck, the webs of the front and interior girders, and along the underside of the deck between the girders.

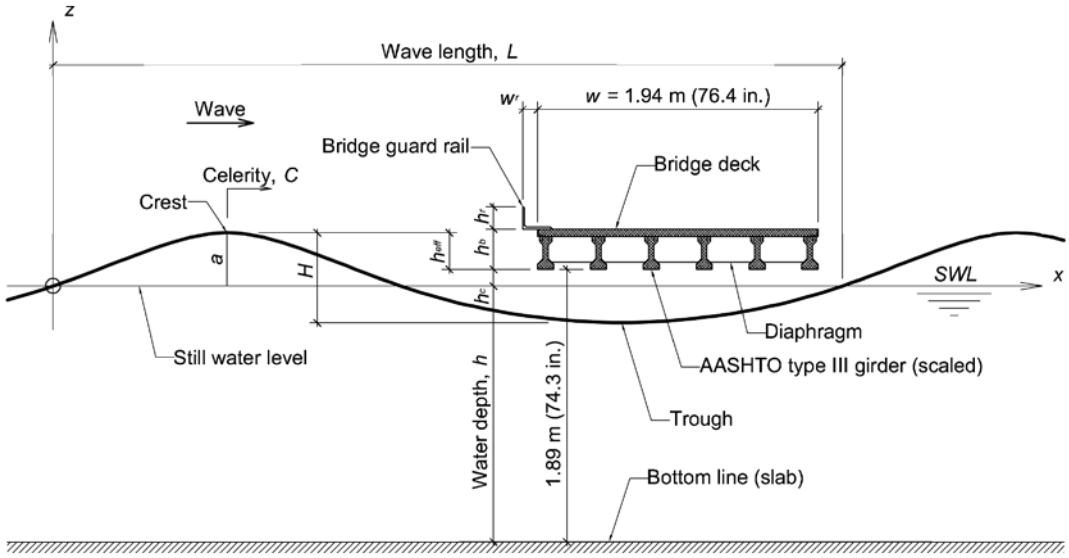

FIG. 4 - ELEVATION VIEW OF THE TEST SPECIMEN ACROSS TANK WITH TEST VARIABLES.

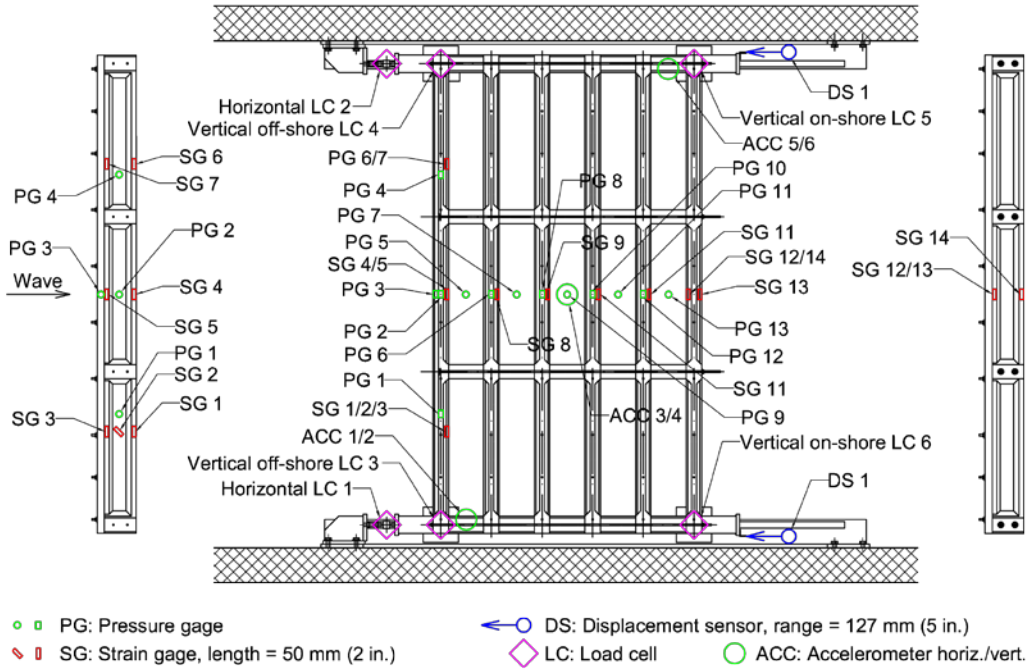

FIG. 5 – PLAN VIEW OF THE TEST SPECIMEN WITH SENSOR DETAILS.

Presented subsequently are example data that were collected for a water depth h of 1.89 m where the still water level is even with the bottom flange of the girders, i.e. $d^* = 0$. Some of the biggest forces are found under these conditions. The waves used in the following examples were regular with target wave period and height of 2.5 s and 0.625 m, respectively. The left side are Phase 1 while the right side are from Phase 2b.

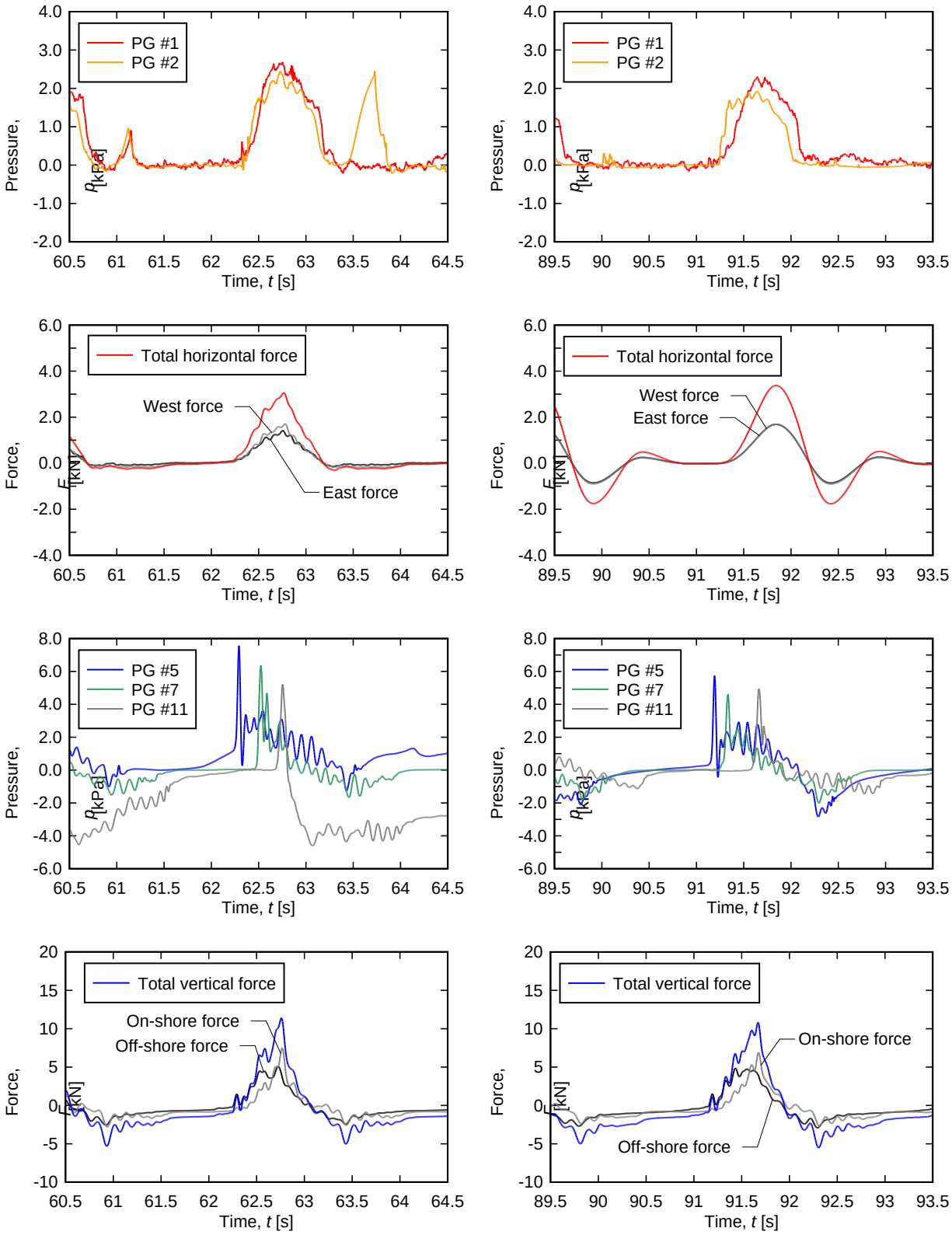

FIG. 6 – EXAMPLE MEASUREMENT FOR PHASE 1 (LEFT COLUMN) AND PHASE 2B (RIGHT COLUMN)

It was observed that the substructure flexibility resulted in higher vertical and horizontal forces than the rigidly attached bridge as summarized in Fig. 7.

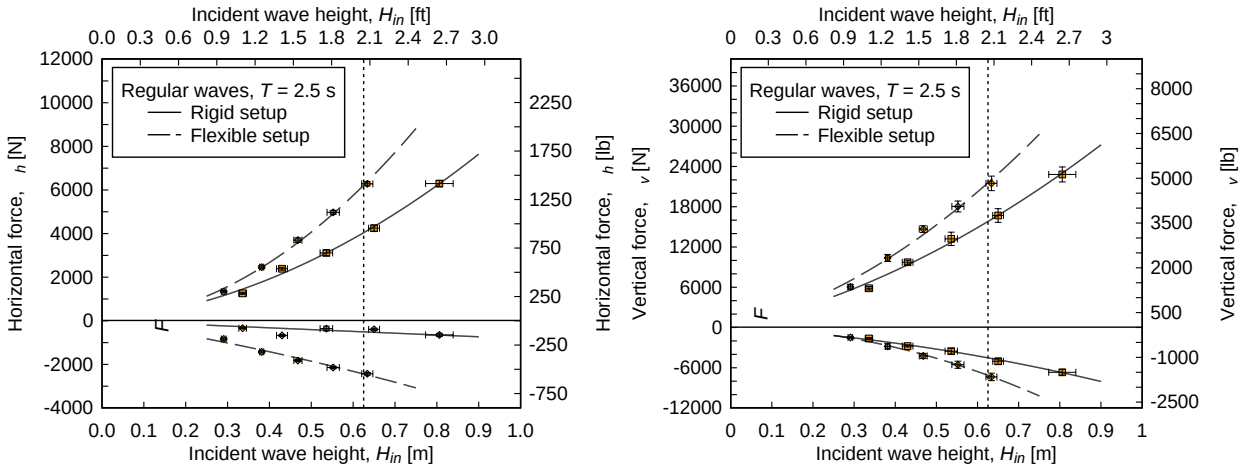

FIG. 7 - MEAN AND ONE STANDARD DEVIATION OF MAXIMUM AND MINIMUM MEASURED FORCES VS. INCIDENT WAVE HEIGHT (HORIZONTAL FORCE ON LEFT SIDE, VERTICAL FORCE ON RIGHT SIDE)

The vertical and horizontal force histories measured on the model were extracted from the ransom wave conditions that represented hurricane wave load conditions similar to Hurricane Katrina in Biloxi Bay, MS as reported by Chen (2009). These were applied to full-scale models of the connections that attach the bridge superstructure to the substructure as described subsequently.

Full-Scale Connection Tests

Wave force effects on the bridge model produced dynamic cyclic uplift with cyclic lateral loads that must be resisted by the connections that anchor the AASHTO type III bridge girders to the pile cap substructure. The simulated wave forces were applied to full-scale test specimens in the laboratory using a novel hybrid-testing method described here.

Prestressed girders have standardized dimensions and were widely used in past practice. The girder specimens were detailed according to in the Florida Department of Transportation plans for the Escambia Bay Bridge. The plans called for two groups of prestressing strands: (18) 13 mm diameter stress relieved straight strand pulled to 112 kN each (6) 13 mm diameter stress relieved double harped strand pulled to 112 kN each. The bursting steel stirrups consist of two L-shaped bars that extend the height of the girder and below the prestressing strand. Fig. 8 shows the reinforcing details at the end of the girder. The length of the specimens was designed to allow both ends of the specimen to be tested separately. The development length of the strand was conservatively assumed to be 0.91 m, and the beam was designed to be 3.05 m, or

approximately three transfer lengths. Thus, if one end of the beam was damaged during a test, there was a middle section of at least one transfer length to fully anchor the strand to enable testing of the opposite end for the second test.

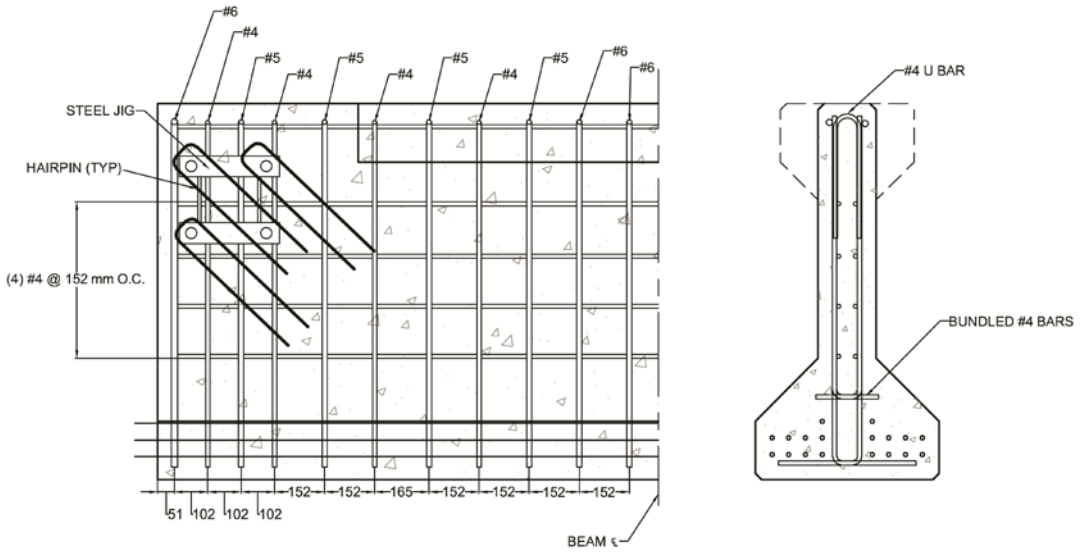

FIG. 8 – ELEVATION VIEWS OF FULL-SCALE GIRDER FOR CONNECTION TEST.

Three commonly used anchorage designs were used in this study. They were: 1) Threaded Insert/Clip Bolt Anchorage (CB), Headed Stud Anchorage (HS), and the Through-Bolt Anchorage (TB). These are shown in Fig. 9. The headed stud anchorage (HS) detail was used at the Escambia Bay, Florida site and failed under hurricane Ivan in 2004. In the case of Escambia Bay, only the exterior girders were detailed with this anchorage.

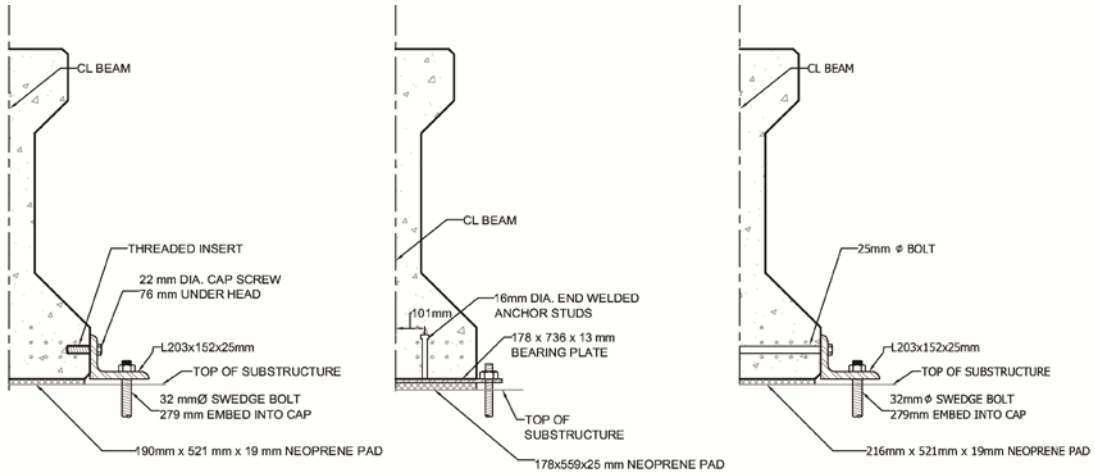

FIG. 9 –CONNECTION DETAILS TESTED (LEFT TO RIGHT: CB, HS, TB).

The specimen loading history was produced by taking the hydraulic model force

histories and scaling them up to prototype scale (the specimen full scale) using Froude similitude, time was multiplied by a factor of $\sqrt{5}$ and force was multiplied by 53. Data taken from the regular wave trial "reg1603" (conditions similar to Hurricane Katrina in Biloxi Bay, MS, reported in Chen (2009)) were used in the present study as the input forcing functions. The wave heights were 0.5 m and 2.5 m for the model and prototype, respectively. The wave periods were 2.68 s and 5.99 s for the model and prototype, respectively. The model data, scaled to prototype scale, were used as the analog input command signal to the hydraulic controllers. When a specimen did not fail at the 100% level, the force magnitudes were increased in 20% increments until failure occurred. Because uplift forces act, the bridge dead load had to be included in the loading history. Using the Escambia Bay Bridge as a prototype, a bridge self-weight load of 178 kN (negative sign) was initially imposed on the girder. This initial applied force represents the tributary weight of components and wearing surface for the exterior girder at the support reaction. Therefore in the data presented subsequently, vertical force values above zero are tensile (when the self-weight precompression is overcome).

The responses shown in this section are for the last imposed time history which produced failure in the connections. The CB connection exhibited the lowest strength of the connection types and failed during the 100% Katrina conditions. The horizontal and vertical load deformation response for the CB anchorage is shown in Fig. 10a and Fig. 11a, respectively. The girder sustained damage around the connection including cracking surrounding the inserts, followed by spalling of the concrete around the inserts, exposure of the outermost prestressing strands along the transfer length. The HS connection exhibited the highest strength of the connection types, failing at 180% of the measured load amplitude under the Katrina conditions. The vertical and horizontal load deformation response for the HS anchorage is shown in Fig. 10b and Fig. 11b, respectively. Failure of the connection was characterized by tensile fracture of the steel headed studs, and large plastic deformations of the connection plate. The damage to the concrete was limited to cracking around the reentrant corners of the plate interface. The TB connection failed at 160% of the measured load amplitude under the Katrina conditions. The vertical and horizontal load deformation response for the TB anchorage is shown in Fig. 10c and Fig. 11c, respectively. Cracking of the girder was observed at 100% Katrina conditions, making the strand susceptible to corrosion. The damage sustained by the girder at failure was extensive. The girder exhibited a large crack across the width of the cross section following the prestressing banding, and once that crack propagated across the entire length, a new crack around the bottom layer of prestressing appeared. The bottom layer of prestressing strand was pulled down and away from the girder as the vertical force produced uplift of the girder.

The test results were compared to the required demands from the recently published AASHTO *Guide Specifications for Bridges Vulnerable to Coastal Storms* (2008). Fig. 12 shows the vertical wave load demands for a bridge span of the type considered in the present research. The vertical load was calculated from the *Guide Specification* and includes the bridge self-weight for a range of maximum wave heights. The calculated maximum load is based on 12 anchorage points per span (one on each end of the girders). Also noted on the figure is the prototype scaled maximum

measured wave induced load from the hydraulic model. Assuming the maximum amount of trapped air, none of the three anchorage designs had sufficient strength to resist the expected vertical loads for wave heights exceeding 3.6 m. In service, bridges with the TB and CB anchorages generally have every girder connected to the pile cap while the Escambia Bay Bridge, with the HS detail, was only anchored at the exterior girders. While anchoring every girder increased the overall bridge resistance, it would not be sufficient to resist the vertical forces prescribed for large wave heights if air is trapped below the bridge deck.

All anchorage types have sufficient strength to resist the horizontal forces if all girders are anchored. The Escambia Bay Bridge, although connected only at the exterior girders with the HS anchorages, would have sufficient strength to resist the prescribed horizontal loads. While the horizontal force component of the wave loading is not as large as the vertical force components, when combined these forces can act in concert to sweep bridges from the substructure upon connection failure dominated by the vertical loading.

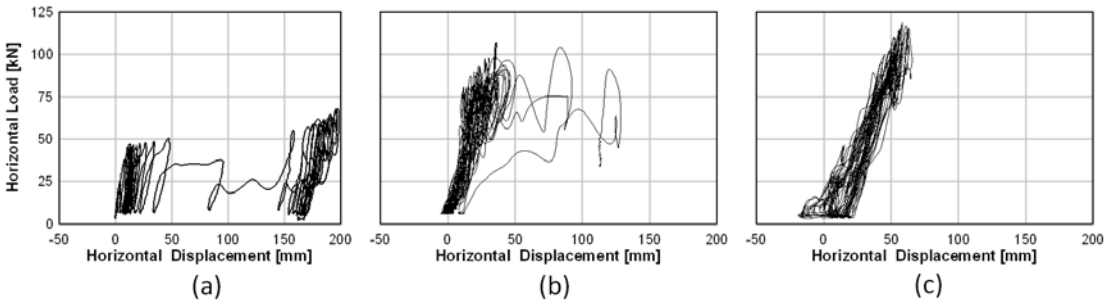

FIG. 10 - HORIZONTAL FORCE-DEFORMATION RESPONSE (LEFT TO RIGHT CB, HS, TB)

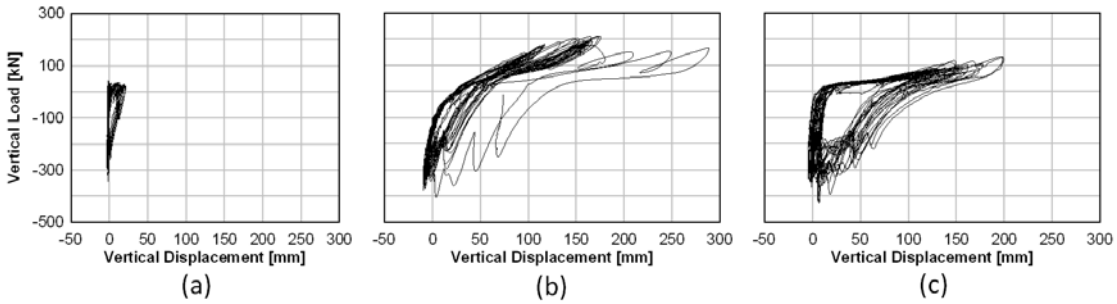

FIG. 11 - VERTICAL FORCE-DEFORMATION RESPONSE (LEFT TO RIGHT CB, HS, TB)

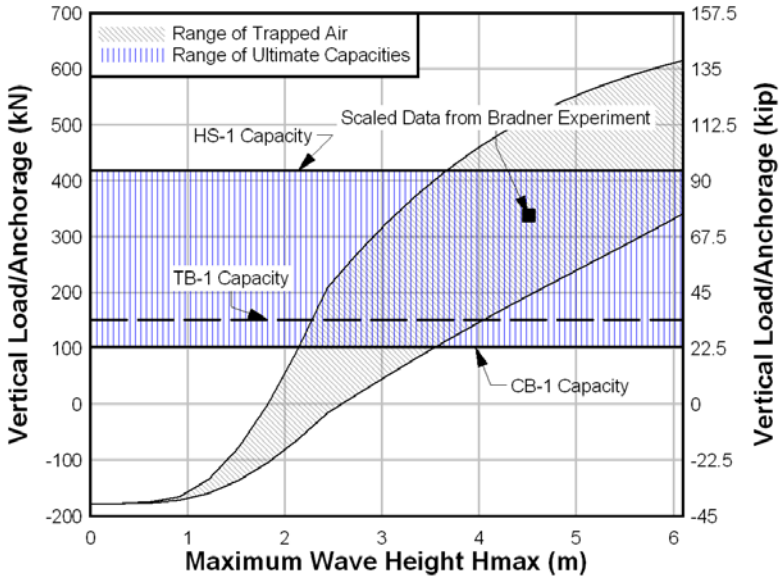

FIG. 12 – VERTICAL LOAD PER ANCHORAGE REQUIRED BY AASHTO GUIDE SPECIFICATION AND RELATIVE ANCHOR CAPACITIES.

Conclusions

Hydro-dynamic tests of a 1:5 scale model of a real highway bridge located on Escambia Bay, Florida were conducted to measure the wave forces on the bridge. The model used an innovative laboratory setup that allowed the test specimen to simulate the dynamic response of the substructure. The flexible substructure produced larger forces on the bridge than if it were rigid. The measured wave force histories on the large-scale hydrodynamic model were converted into the vertical and horizontal force components applied to the connections that join the superstructure to the substructure. The force histories from the large-scale hydrodynamic model were increased to prototype scale and then applied to full-size connection elements to characterize the structural performance. Three commonly used connection details were tested. The wave loading produced damage in the girders and the capacity of the connections would not be sufficient to resist the vertical loads prescribed by the AASHTO *Guide Specification* for the bridge configuration considered when wave heights exceeded 3.6 m and significant trapped air is present. The testing methods developed represent a new technique in hybid testing to investigate fluid-structure interactions. Additional details can be found in Lehrman *et al*. (2012) and Bradner *et al*. (2011)

Acknowledgments

This research was funded by Oregon Transportation Research and Education Consortium (OTREC) and the National Science Foundation with grant CMMI 0800822 of the Hazard Mitigation and Structural Engineering program. Dr. Keith Kaufman of Knife River in Harrisburg, OR, Mr. Robbie Chambless of the Alabama Department of Transportation, Mr. Artur D'Andrea of the Louisiana Department of Transportation, and Mr. Rick Renna of the Florida Department of Transportation provided helpful

suggestions. The findings, conclusions and recommendations presented are those of the authors and do not necessarily reflect the views of the project sponsors or individuals acknowledged.

References

American Assoc. of State Highway and Transp. Officials (2008). "Guide Specification for Bridges Vulnerable to Coastal Storms." 1st Ed., Washington, DC.

Bea, R. G., Iversen, R., and Xu, T. (2001). "Wave-in-Deck Forces on Offshore Platforms." J of Offshore Mechanics and Arctic Eng. , Vol. 123, Feb. 2001, 10-21.

Bradner, C., Schumacher, T., Cox, D., and C. Higgins (2011). "Experimental Setup for a Large-Scale Bridge Superstructure Model Subjected to Waves." J. Waterway, Port, Coastal, Ocean Eng., 137(1), 3–11.

Chen, Q., Wang, L., & H. Zhao, (2009). "Hydrodynamic Investigation of Coastal Bridge Collapse during Hurricane Katrina," J. of Hydraulic Eng., 135 (3), 175-186.

Cuomo, G., Tirindelli, M., and Allsop, W. (2007), "Wave-in-deck loads on exposed jetties." Coastal Engineering, Vol. 54, Issue 9, September 2007, 657-679.

Denson, K. H. (1980). Wave Forces on Causeway-Type Coastal Bridges: Effects of Angle of Wave Incidence and Cross-Section Shape, Water Resources Research Institute, Mississippi State University.

Douglass, S., Chen, Q., & J. Olsen (2006). "Wave Forces on Bridge Decks - Draft Report," Coastal Transportation Engineering Research and Education Center. University of South Alabama

Lehrman, J., Higgins, C., and Cox, D. (2012). "Performance of Highway Bridge Girder Anchorages under Simulated Hurricane Wave Induced Loads." J. Bridge Eng., 17(2), 259–271.

Marin, J., & M. Sheppard, (2009). "Storm Surge and Wave Loading on Bridge Superstructures," Proceedings of Structures Congress, Austin, TX. pp. 557-566.

Padgett, J., DesRoches, R., Nielson, B., Yashinsky, M., Kwon, O., Burdette, N., and Tavera, E. (2008). "Bridge Damage and Repair Costs from Hurricane Katrina." J. Bridge Eng., 13(1), 6–14.

Robertson, I., Riggs, H., Yim, S., and Y. Young, (2007). "Lessons from Hurricane Katrina Storm Surge on Bridges and Buildings," J. of Waterway, Port, Coastal, and Ocean Engineering, 133 (6), 463-483.